A Journal of the Gesellschaft Deutscher Chemiker

Angewandte International Edition GDCh Chemie

www.angewandte.org

Accepted Article

Title: A Systematic Study of Unsaturation in Lipid Nanoparticles Leads to Improved mRNA Transfection In Vivo

Authors: Sang Lee, Qiang Cheng, Xueliang Yu, Shuai Liu, Lindsay Johnson, and Daniel John Siegwart

To be cited as: *Angew. Chem. Int. Ed.* 10.1002/anie.202013927

Link to VoR: https://doi.org/10.1002/anie.202013927

WILEY-VCH

COMMUNICATION

A Systematic Study of Unsaturation in Lipid Nanoparticles Leads to Improved mRNA Transfection In Vivo

Sang M. Lee, Qiang Cheng, Xueliang Yu, Shuai Liu, Lindsay T. Johnson, Daniel J. Siegwart*

S.M. Lee, Dr. Q. Cheng. Dr. X. Yu, Dr. S. Liu, L.T. Johnson, Professor D.J. Siegwart
Department of Biochemistry
University of Texas Southwestern Medical Center
5323 Harry Hines Blvd., Dallas, Texas, 75390-9038 (USA)
Email: daniel.siegwart@utsouthwestern.edu

Supporting information for this article is given via a link at the end of the document.

Abstract: Lipid nanoparticles (LNPs) represent the leading concept for mRNA delivery. Unsaturated lipids play important roles in nature with potential for mRNA therapeutics but are difficult to access through chemical synthesis. To systematically study the role of unsaturation, modular reactions were utilized to access a library of 91 amino lipids, enabled by the synthesis of unsaturated thiols. An ionizable lipid series (4A3) emerged from *in vitro* and *in vivo* screening, where the 4A3 core with a citronellol-based (Cit) periphery emerged as best. We studied the interaction between LNPs and a model endosomal membrane where 4A3-Cit demonstrated superior lipid fusion over saturated lipids, suggesting its unsaturated tail promotes endosomal escape. Furthermore, 4A3-Cit significantly improved mRNA delivery efficacy *in vivo* via Selective ORgan Targeting (SORT), resulting in 18-fold increased protein expression over parent LNPs. These findings provide insight into how lipid unsaturation promotes mRNA delivery and demonstrate how lipid mixing can enhance efficacy.

Beyond functioning as a link between the genetic code of DNA and functional proteins, messenger mRNA (mRNA) has emerged as a versatile tool to produce proteins for therapeutic applications towards cancer, vaccines, and other areas.[1] However, the major challenge of RNA therapeutics remains efficacious delivery. mRNAs are incapable of passing through cellular membranes on their own due to their physiochemical attributes and propensity for degradation. Methods are needed to encapsulate and deliver mRNA inside cells.[2] To address this challenge, lipid nanoparticles (LNPs) represent the leading concept for mRNA delivery. LNPs are composed of multiple lipids, including ionizable amino lipids, which acquire charge during endosomal maturation and allow endosomal escape of RNA into the cytoplasm to enable delivery of the genetic material.[3]

LNPs were initially established as carriers for siRNAs,[4] and have increasingly been explored for delivery of mRNA.[1a, 5] Studies have shown that optimization of LNP carriers for mRNA versus siRNA often require chemical changes to the lipids involved,[4c, 6] as well as the molar relationship of lipids that compose of the formulations.[7] Despite this progress, much remains unknown about structure-activity relationships (SAR) uniting chemistry and efficacy for mRNA delivery. Recently, the field of mRNA therapeutics has started to include unsaturated lipids in LNPs in the form of natural unsaturated fatty acids and its motifs.[8] In nature, unsaturated lipids play a pivotal role in maintaining the stability and fluidity of membranes.[9] The universal importance of unsaturated lipids in natural membranes support a LNP design emulating such a chemical composition. However, there has been no robust study on the optimization of unsaturation for LNPs nor its purpose.

To study the role of unsaturated lipids in LNPs, we focused on an ionizable amino lipid platform created using modular dendrimer growth reactions, where we could systematically introduce unsaturation. Our lipid design consisting of an ionizable amine core, ester-based degradable linker, and alkyl thiol tail periphery[10] was revisited with attention on unsaturation for the periphery. To incorporate unsaturation into the ionizable lipid, we synthesized alkenyl thiols and inserted them as the hydrophobic tail domain, mimicking natural fatty acids. These newly synthesized lipids were formulated into LNPs and compared to their saturated parents. In doing so, we aimed to understand why unsaturation may be important for LNPs and explore the potential applications of unsaturated LNPs.

Modular reactions were utilized to create a chemically diverse library of unsaturated amino lipids. Our synthetic route towards the ionizable lipid involves a nucleophilic amine addition to an ester-based linker, followed by a Michael addition with the thiols. Previous studies solely involved alkyl thiols because unsaturated thiols are not commercially available. Thus, we hypothesized bridging this gap by synthesizing unsaturated thiols from alkenyl alcohols and terpenes found in nature (**Scheme 1A**). However, initial attempts for the unsaturated thiols proved difficult, resulting in undesired products and low yields.

After employing multiple strategies, including the Mitsunobu reaction/reduction and Bunte salt, two methods emerged as optimal based on the alcohol, reaction scale, and yield (**Figure S1**). For most allylic alcohols, conversion of the alcohol to a bromide and subsequent reaction with NaSH provided thiols at 48% to 91% yield. For non-allylic alcohols and farnesol, tosyl protection of the alcohol and subsequent treatment with NaSH afforded the desired thiols at 19% to 67% yields. Thiol nomenclature was based on the carbon chain length (6/8), position of unsaturation (2-5), configuration (cis/trans), and/or their natural product derivative (Citronellol, Nerol, and Farnesol). In tandem, seven ionizable amines were selected as candidates based on the established optimal pKa of 6.2-6.5 for ionizable lipids.[11] The amines were prepared by reacting with an ester-based linker synthesized as previously described.[10] With the amine cores and thiols in hand, appropriate equivalents of thiols per amine were combined with the modified amines and dimethyl phenyl pyridine as a catalyst to create the desired ionizable, unsaturated lipids (**Scheme 1B**).

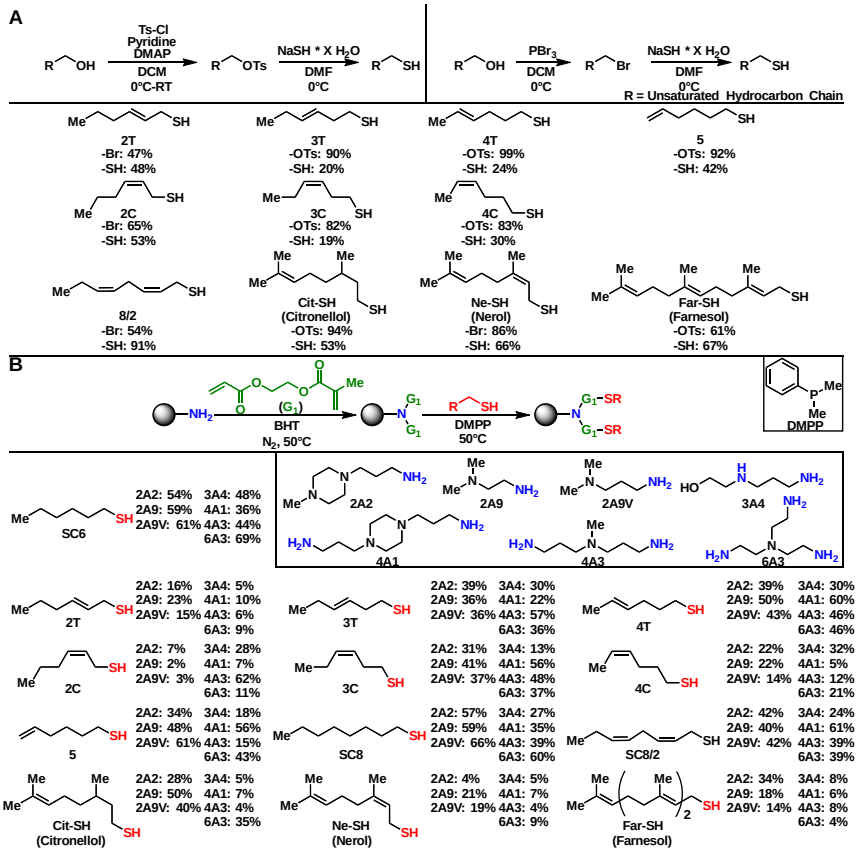

Scheme 1. Synthesis of unsaturated thiols allowed access to unsaturated lipids. **A)** Scheme and reaction scope for synthesis of alkenyl thiols using non-allylic and allylic alcohols. **B)** Scheme and reaction scope for synthesis of ionizable amino lipids using 7 different amine cores with isolated yields reported.

The new lipids were formulated into LNPs using a mix of the synthesized lipid, DOPE, cholesterol, and DMG-PEG2k (15:15:30:3, mol:mol), encapsulating Firefly Luciferase (Luc) mRNA. This ratio was selected based on parameters previously optimized for mRNA delivery.[7c] We evaluated the LNPs in IGROV-I cells (25 ng/well) for cell viability and Luc expression (**Figure 1**). Assessment of the heat map allowed for determination of SARs with respect to hydrophobic domain and amine core chemical structure. While introducing unsaturation in the tail produced some lipids with improved transfection over parent compounds, this chemical alteration was not a change that automatically and universally improved performance. Rather, the placement and *cis*/*trans* configuration of the unsaturation were important in determining whether *in vitro* mRNA delivery would be improved. For example, 8/2 showed comparable Luc expression to its saturated counterpart (SC8). Among all cores examined in the initial screen, 4A3 was the most efficacious. Therefore, we selected the entirety of the 4A3 series to further evaluate its capabilities and study SAR with respect to the hydrophobic domain.

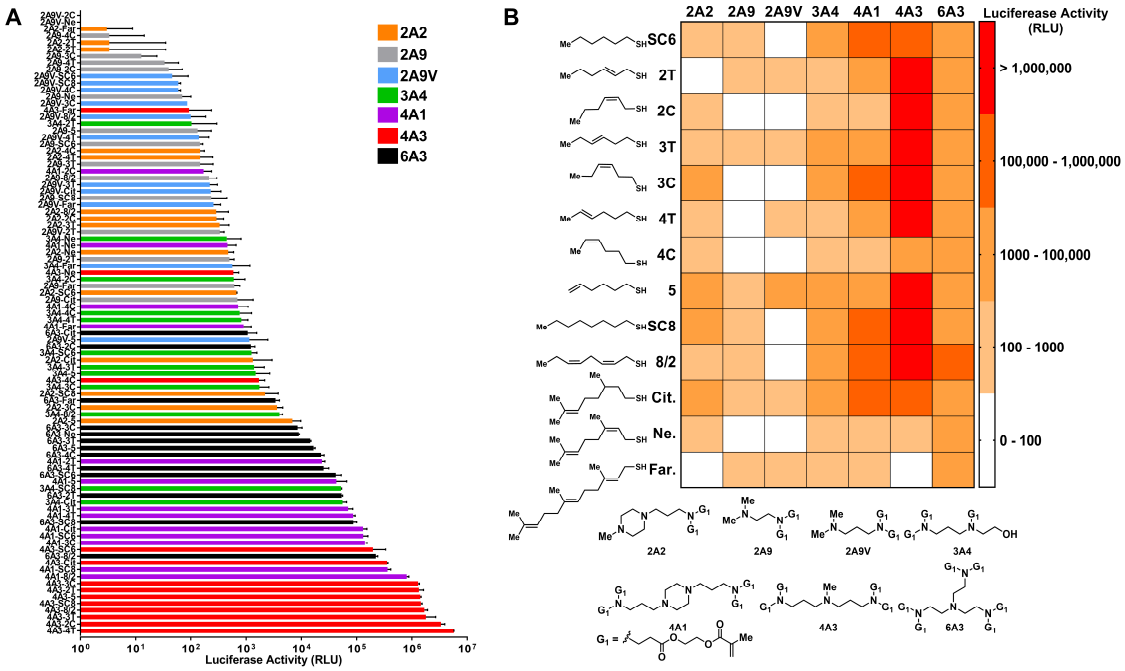

Figure 1. 4A3-derived lipids performed best across the lipid series for Luc mRNA delivery to IGROV-I cells. **A)** Bar graph of the *in vitro* Luc expression assay shows 4A3-4T as the most potent. **B)** Heat map of the *in vitro* Luciferase assay data revealed differences based on position and configuration of the unsaturation.

Next, we evaluated the 4A3 series to assess how the unsaturation variations affected mRNA delivery *in vivo*, which is the more relevant setting for mRNA therapeutic testing. LNPs were formulated using the same components for *in vitro* testing in the same molar ratio as described above. C57BL/6 mice were administered with each of the 4A3-based LNP series carrying Luc mRNA via tail-vein injections (**Figure 2**). Clear differences from the *in vitro* data appeared. While the six-carbon chain series showed few significant differences amongst each other, the eight-carbon tail series exhibited striking distinctions.

Despite being structurally similar, 4A3-Cit performed better than 4A3-Ne, differing only by a prenyl motif per tail. This disparity is likely due to the increased rigidity based on this structural difference. The comparison of the duo suggests that the "stiffness" of the components and its ability to promote membrane permeability may be an important factor in improving mRNA delivery when tailoring to its unsaturation. With 4A3-8/2, it exhibited lower Luc expression compared to its alkyl partner, suggesting again that the introduction of unsaturation alone is not sufficient to increase efficacy. Efficacy did not significantly correlate with size, PDI, or encapsulation efficiency (**Figure S5**), suggesting that chemical structure was the major driver of efficacy. Moreover, the introduction of unsaturation did not change the biodistribution of 4A3-SC8 and saturated 4A3-Cit based LNPs (**Figure S8**). As endosomal escape of LNPs remains a major challenge that correlates with amino lipid chemistry, we postulated that these LNPs may differ based on their ability to escape the endosome.[3]

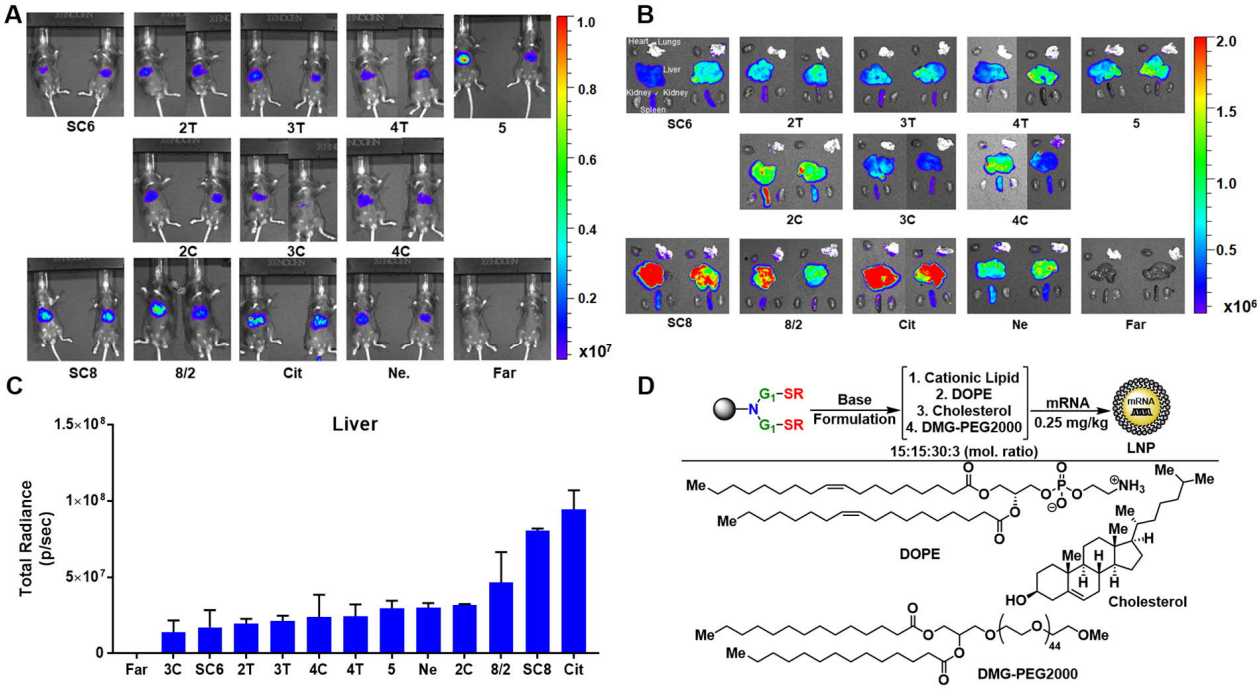

Figure 2. *Ex vivo* imaging shows highest mRNA expression in eight carbon series (0.25 Luc mg/kg). **A)** Whole body images 6 hours after i.v. administration of LNPs. **B)** *Ex vivo* organs imaged 6 hours after administration of LNPs. **C)** Quantified total radiance of the liver. **D)** Representation of the 4-component standard LNP *in vivo* formulation method.

To gain mechanistic insight into this foray, the following assay was conducted to study how our LNPs interacted with a model endosomal membrane. We employed a fluorescence resonance energy transfer (FRET)-based assay to determine the LNP's ability to disrupt and fuse with the endosomal membrane (**Figure 3**). DOPE-conjugated FRET probes (NBD-PE and N-Rh-PE) were formulated into endosome-mimicking nanoparticles. NBD is normally quenched by the rhodamine, but the NBD signal would rise if disruption of the membrane occurred.. In accordance with the *in vivo* data, 4A3-Cit proved to be the best. As citronellol is a known membrane disrupter, we believe 4A3-Cit's unique structure promotes better endosomal escape than the other LNPs.[12]

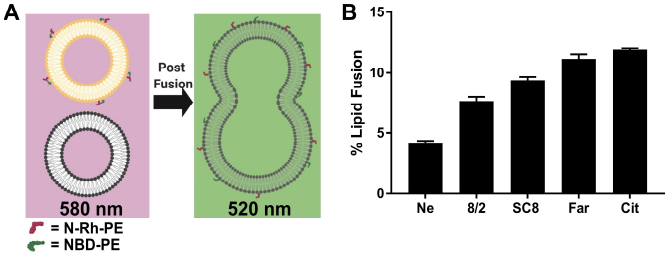

Figure 3. A lipid fusion assay shows 4A3-Cit with the highest lipid fusion percent. **A)** Visual assay representation showing the emission changes based on fusion. **B)** Percent of lipid fusion of LNPs with the model endosomal membrane.

To further examine cellular uptake and intracellular trafficking, we performed *in vitro* experiments using Cy5-labeled mRNA LNPs. The results showed that 4A3-SC8, 4A3-Far, and 4A3-Cit LNPs are all effectively internalized at 4 hours and 24 hours (**Figure S10 A** and **B**). There were differences at 4 hours, with the two unsaturated lipids (4A3-Far and 4A3-Cit) LNPs internalizing slightly faster than the saturated (4A3-SC8) LNPs. We further tracked the progression of Cy5 mRNA from the cell membrane to endosomes to lysosomes and quantified co-localization of Cy5 mRNA with lysosomes. Interestingly, there was significantly higher colocalization between 4A3-Far and lysosomes compared to 4A3-SC8 and 4A3-Cit. These results suggest that 4A3-Far LNPs lead to mRNA accumulation in lysosomes and unproductive delivery. Moreover, the reduced colocalization with lysosomes for 4A3-SC8 and 4A3-Cit LNPs helps to explain why they are efficacious. The overall results connect chemical structure to factors including cellular uptake, endosomal escape, and intracellular trafficking.

Building on the discovery of unsaturated 4A3-Cit and understanding of increased lipid fusion, we sought to explore how 4A3-Cit could be used to enhance mRNA delivery *in vivo* to the liver. We recently reported a technology called Selective Organ Targeting Nanoparticles (SORT) for selective mRNA delivery to different tissues.[13] In one application, mixing two ionizable lipids into a 5-component LNP increased delivery efficacy to the liver. [13a, 14] We hypothesized that 4A3-SC8 and 4A3-Cit could be combined into a SORT LNP to engineer improved lipid formulations for the liver. We previously showed that mRNA delivery efficacy and tissue tropism correlated with the chemical identity and percent incorporation of the added SORT molecule while keeping the molar amount of other molecules constant. We hypothesized increasing the occupied percentage of our unsaturated lipid would promote endosomal escape and improve mRNA delivery. Thus, the following primary formulations were devised: 4A3-SC8 with additional parent lipid, 4A3-Cit with additional parent lipid, and a mixture of the two lipids where one would serve as the parent lipid and the other served as additional supplemental SORT lipid (**Figure S2**).

First, we aimed to optimize the SORT lipid required to improve mRNA transfection by evaluating formulations across a range of SORT lipid amounts. Additional 4A3-SC8 yielded only mild improvements (**Figure S3**), but formulations involving additional Cit achieved significant improvements (**Figure 4**). Once we identified the ideal percentages for the SORT lipids (+5 % SC8 and +20/30% of Cit), we tested the cross-over mixtures. Cit+SC8 (5%) performed only slightly better than its parent formulation (**Figure S3**), but SC8+Cit (20%) surpassed all others with an 18-fold increase of the average luminescence. SC8+Cit (20%) was also superior to its saturated parent lipid and established benchmarks including 5A2-SC8 LNPs and DLin-MC3-DMA LNPs (**Figure S9**). Interestingly, 8+Cit (30%) performed worse than its Cit (+30%) counterpart, and the reverse was observed with its 20% variant. The data revealed that improvement is accessible by increasing occupancy of the 4A3-Cit, but there is a threshold for the additive effect of Cit. The comparison of the average luminescence suggests that there needs to be a careful balance of ionizable lipids for LNPs to achieve successful increased transfection.

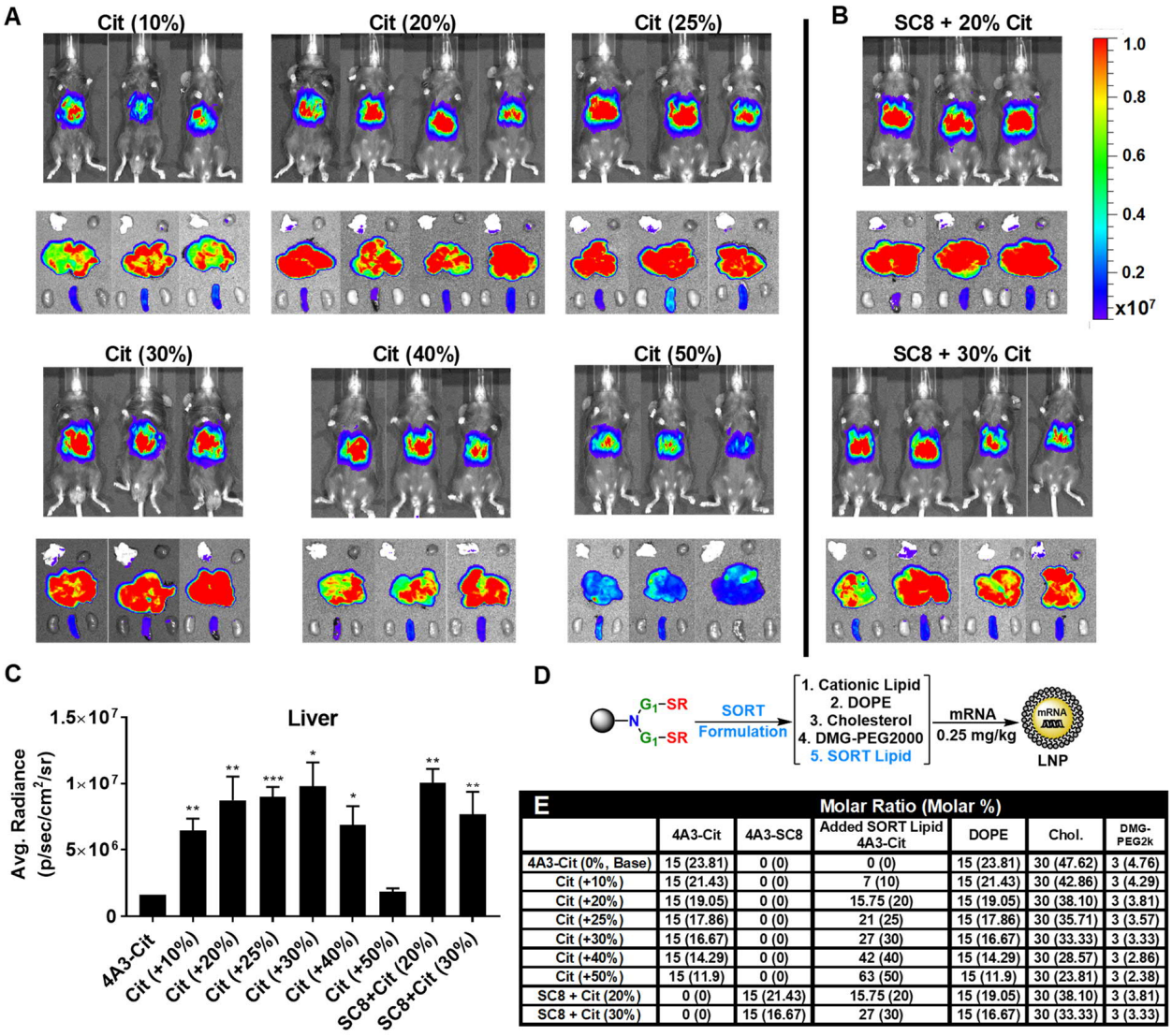

E

Molar Ratio (Molar %)						
	4A3-Cit	4A3-SC8	Added SORT Lipid 4A3-Cit	DOPE	Chol.	DMG-PEG2k
4A3-Cit (0%, Base)	15 (23.81)	0 (0)	0 (0)	15 (23.81)	30 (47.62)	3 (4.76)
Cit (+10%)	15 (21.43)	0 (0)	7 (10)	15 (21.43)	30 (42.86)	3 (4.29)
Cit (+20%)	15 (19.05)	0 (0)	15.75 (20)	15 (19.05)	30 (38.10)	3 (3.81)
Cit (+25%)	15 (17.86)	0 (0)	21 (25)	15 (17.86)	30 (35.71)	3 (3.57)
Cit (+30%)	15 (16.67)	0 (0)	27 (30)	15 (16.67)	30 (33.33)	3 (3.33)
Cit (+40%)	15 (14.29)	0 (0)	42 (40)	15 (14.29)	30 (28.57)	3 (2.86)
Cit (+50%)	15 (11.9)	0 (0)	63 (50)	15 (11.9)	30 (23.81)	3 (2.38)
SC8 + Cit (20%)	0 (0)	15 (21.43)	15.75 (20)	15 (19.05)	30 (38.10)	3 (3.81)
SC8 + Cit (30%)	0 (0)	15 (16.67)	27 (30)	15 (16.67)	30 (33.33)	3 (3.33)

Figure 4. 4A3-SC8 + Cit (20%) improved Luc mRNA expression in liver 18-fold over the saturated base LNP formulation (4A3-Cit). **A)** Optimization of Cit SORT lipid. **B)** Evaluation of cross-over mix using the identified lipids percentages. **C)** Quantified average luminescence of the liver after 6 hours. **D)** Molar ratio and percentage of the 5-component SORT LNP formulations. **D)** Visual representation of formulation. **E)** Table of details for the base LNP and SORT LNP formulations (Total lipids/mRNA ratio = 40; wt/wt).

In summary, we synthesized unsaturated thiols that enabled access to a library of 91 ionizable lipids. *In vitro* mRNA delivery screening results revealed differences and SAR that correlated with the location/configuration of the unsaturated bond(s) rather than the simple presence of unsaturation. Selecting the 4A3 amine core to study *in vivo*, 4A3-Cit demonstrated the highest efficacy. Mechanistic studies using model endosomal membranes indicated that 4A3-Cit demonstrated the highest lipid fusion ability, suggesting its unique tail structure may enhance endosomal escape. 4A3-Cit further established its exceptional utility for mRNA delivery through application in SORT LNPs. SC8+Cit (20%) SORT LNPs improved mRNA delivery 18-fold over parent formulations. The findings from this work aid a deeper understanding of how unsaturation may promote mRNA delivery by increasing endosomal fusion, identify 4A3-Cit as a potent new lipid, and further expand the utility of SORT LNPs for efficacious mRNA delivery.

Acknowledgements. D.J.S. acknowledges financial support from the National Institutes of Health (NIH) National Institute of Biomedical Imaging and Bioengineering (NIBIB) (R01 EB025192-01A1), the Cystic Fibrosis Foundation (CFF) (SIEGWA18XX0), the Cancer Prevention and Research Institute of Texas (CPRIT) (RP190251), the American Cancer Society (ACS) (RSG-17-012-01), and the Welch Foundation (I-1855). We acknowledge the UTSW Small Animal Imaging Shared Resource (NIH NCI P30CA142543). S.M.L. acknowledges support from NIH (T32GM127216).

Keywords: lipid nanoparticles • mRNA • unsaturated lipids • unsaturated thiols • nanomaterials

References

[1] a) K. A. Hajj, K. A. Whitehead, *Nat. Rev. Mater.* **2017**, *2*, 17056; b) N. Pardi, M. J. Hogan, F. W. Porter, D. Weissman, *Nat. Rev. Drug Discovery* **2018**, *17*, 261-279; c) P. S. Kowalski, A. Rudra, L. Miao, D. G. Anderson, *Mol. Ther.* **2019**, *27*, 710-728.

[2] a) U. Sahin, K. Kariko, O. Tureci, *Nat. Rev. Drug Discovery* **2014**, *13*, 759-780; b) T. Wei, Q. Cheng, L. Farbiak, D. G. Anderson, R. Langer, D. J. Siegwart, *ACS Nano* **2020**, *14*, 9243-9262; c) Y. Lyu, D. Cui, H. Sun, Y. Miao, H. Duan, K. Pu, *Angew. Chem. Int. Ed.* **2017**, *56*, 9155-9159; d) Y. Lyu, S. He, J. Li, Y. Jiang, H. Sun, Y. Miao, K. Pu, *Angew. Chem. Int. Ed.* **2019**, *58*, 18197-18201.

[3] A. Wittrup, A. Ai, X. Liu, P. Hamar, R. Trifonova, K. Charisse, M. Manoharan, T. Kirchhausen, J. Lieberman, *Nat. Biotechnol.* **2015**, *33*, 870-876.

[4] a) K. Whitehead, R. Langer, D. Anderson, *Nat. Rev. Drug Discovery* **2009**, *8*, 129-138; b) R. Kanasty, J. R. Dorkin, A. Vegas, D. Anderson, *Nat. Mater.* **2013**, *12*, 967-977; c) J. B. Miller, D. J. Siegwart, *Nano Res.* **2018**, *11*, 5310-5337; d) A. Akinc, M. A. Maier, M. Manoharan, K. Fitzgerald, M. Jayaraman, S. Barros, S. Ansell, X. Du, M. J. Hope, T. D. Madden, B. L. Mui, S. C. Semple, Y. K. Tam, M. Ciufolini, D. Witzigmann, J. A. Kulkarni, R. van der Meel, P. R. Cullis, *Nat. Nanotechnol.* **2019**, *14*, 1084-1087.

[5] a) K. J. Kauffman, M. J. Webber, D. G. Anderson, *J. Controlled Release* **2016**, *240*, 227-234; b) J. Li, Y. He, W. Wang, C. Wu, C. Hong, P. T. Hammond, *Angew. Chem. Int. Ed.* **2017**, *56*, 13709-13712; c) S. Ramishetti, I. Hazan-Halevy, R. Palakuri, S. Chatterjee, S. Naidu Gonna, N. Dammes, I. Freilich, L. Kolik Shmuel, D. Danino, D. Peer, *Adv. Mater.* **2020**, *32*, e1906128; d) C. D. Sago, M. P. Lokugamage, K. Paunovska, D. A. Vanover, C. M. Monaco, N. N. Shah, M. Gamboa Castro, S. E. Anderson, T. G. Rudoltz, G. N. Lando, P. Munnilal Tiwari, J. L. Kirschman, N. Willett, Y. C. Jang, P. J. Santangelo, A. V. Bryksin, J. E. Dahlman, *Proc. Natl. Acad. Sci. U.S.A.* **2018**, *115*, E9944-E9952; e) H. Xiong, S. Liu, T. Wei, Q. Cheng, D. J. Siegwart, *J. Controlled Release* **2020**, *325*, 198-205; f) Y. Wang, J. Tang, Y. Yang, H. Song, J. Fu, Z. Gu, C. Yu, *Angew. Chem. Int. Ed.* **2020**, *59*, 2695-2699; g) X. Zhao, J. Chen, M. Qiu, Y. Li, Z. Glass, Q. Xu, *Angew. Chem. Int. Ed.* **2020**.

[6] J. B. Miller, S. Zhang, P. Kos, H. Xiong, K. Zhou, S. S. Perelman, H. Zhu, D. J. Siegwart, *Angew. Chem. Int. Ed.* **2017**, *56*, 1059-1063.

[7] a) K. J. Kauffman, J. R. Dorkin, J. H. Yang, M. W. Heartlein, F. DeRosa, F. F. Mir, O. S. Fenton, D. G. Anderson, *Nano Lett.* **2015**, *15*, 7300-7306; b) B. Li, X. Luo, B. Deng, J. Wang, D. W. McComb, Y. Shi, K. M. Gaensler, X. Tan, A. L. Dunn, B. A. Kerlin, Y. Dong, *Nano Lett.* **2015**, *15*, 8099-8107; c) Q. Cheng, T. Wei, Y. Jia, L. Farbiak, K. Zhou, S. Zhang, Y. Wei, H. Zhu, D. J. Siegwart, *Adv. Mater.* **2018**, *30*, e1805308.

[8] a) O. S. Fenton, K. J. Kauffman, R. L. McClellan, J. C. Kaczmarek, M. D. Zeng, J. L. Andresen, L. H. Rhym, M. W. Heartlein, F. DeRosa, D. G. Anderson, *Angew. Chem. Int. Ed.* **2018**, *130*, 13770-13774; b) X. F. Zhang, W. Y. Zhao, G. N. Nguyen, C. X. Zhang, C. X. Zeng, J. Y. Yan, S. Du, X. C. Hou, W. Q. Li, J. Jiang, B. B. Deng, D. W. McComb, R. Dorkin, A. Shah, L. Barrera, F. Gregoire, M. Singh, D. L. Chen, D. E. Sabatino, Y. Z. Dong, *Science Adv.* **2020**, *6*.

[9] P. J. Quinn, F. Joo, L. Vigh, *Prog. Biophys. Mol. Bio.* **1989**, *53*, 71-103.

[10] K. Zhou, L. H. Nguyen, J. B. Miller, Y. Yan, P. Kos, H. Xiong, L. Li, J. Hao, J. T. Minnig, H. Zhu, D. J. Siegwart, *Proc. Natl. Acad. Sci. U.S.A.* **2016**, *113*, 520-525.

[11] M. Jayaraman, S. M. Ansell, B. L. Mui, Y. K. Tam, J. X. Chen, X. Y. Du, D. Butler, L. Eltepu, S. Matsuda, J. K. Narayanannair, K. G. Rajeev, I. M. Hafez, A. Akinc, M. A. Maier, M. A. Tracy, P. R. Cullis, T. D. Madden, M. Manoharan, M. J. Hope, *Angew. Chem. Int. Ed.* **2012**, *51*, 8529-8533.

[12] M. Kopecna, M. Machacek, A. Novackova, G. Paraskevopoulos, J. Roh, K. Vavrova, *Sci. Rep.* **2019**, *9*.

[13] a) Q. Cheng, T. Wei, L. Farbiak, L. T. Johnson, S. A. Dilliard, D. J. Siegwart, *Nat. Nanotechnol.* **2020**, *15*, 313-320; b) T. Wei, Q. Cheng, Y. L. Min, E. N. Olson, D. J. Siegwart, *Nat. Commun.* **2020**, *11*, 3232.

[14] L. Miao, J. Lin, Y. Huang, L. Li, D. Delcassian, Y. Ge, Y. Shi, D. G. Anderson, *Nat. Commun.* **2020**, *11*, 2424.

10.1002/anie.202013927

Entry for the Table of Contents

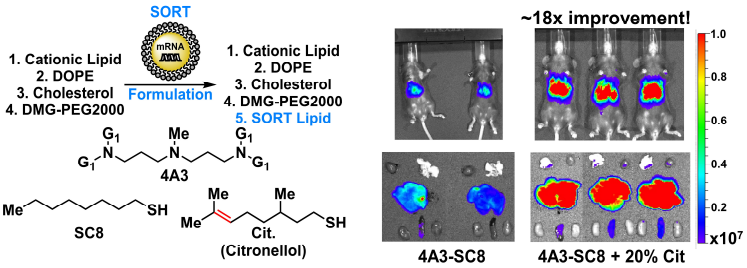

Unsaturated amino lipids were synthesized to study the role of unsaturation in lipid nanoparticle (LNP)-mediated mRNA delivery. A lipid series with a Citronellol tail (4A3-Cit) was identified from a library screen. Employing 4A3-Cit in new Selective ORgan Targeting (SORT) formulation resulted in an 18-fold increase in mRNA expression over saturated LNPs. The findings provide insights to how unsaturation and SORT mixing can promote mRNA delivery.

Institute and/or researcher Twitter usernames: @DJSiegwart